

Analytical formulas of beam deflection due to vertical temperature difference

Yi ZHOU^{1, 2,*}, Yong XIA^{2,*}, Yozo FUJINO³

¹Beijing Key Laboratory of Urban Underground Space Engineering, University of Science & Technology Beijing, Beijing 100083, China

²Department of Civil and Environmental Engineering, The Hong Kong Polytechnic University, Hong Kong, China

³Institute of Advanced Sciences, Yokohama National University, Yokohama 240-8501, Japan

* Corresponding authors: zhouyi@ustb.edu.cn (Y. Zhou); ceypia@polyu.edu.hk (Y. Xia)

Abstract

This paper presents unified analytical formulas to calculate the vertical temperature difference induced deflection of a prismatic beam with any number of spans. The influences of the structural geometry, material property, and temperature change on the beam deflection ~~is~~ are investigated through detailed parametric analysis. A beam with odd-numbered spans has distinct thermal deformation characteristics from that with even-numbered spans. For an equal-span continuous beam, the outermost spans on both ends undergo the largest deformation due to the vertical temperature difference, while the middlemost spans the least. The mid-span deflection of each span converges quickly to the limit value with the increase of the total span number n . The limits for the outermost and middlemost spans are respectively $D_0 \cdot (\sqrt{3} - 1) / 2$ and zero, where D_0 is the thermal deflection at mid-span of a simply supported beam with the same span length. ~~This study proposes simple and exact formulas to compute the thermal deformation of beams, and also has far-reaching implications on the deflection-based structural health monitoring.~~ This study enhances the understanding of the thermal behaviour of beams.

Keywords

Beam; vertical temperature difference; deflection; analytical formula; mechanism

1 Introduction

Civil structures are always subjected to the cyclic temperature change due to the sunlight exposure,

season alteration, etc. The field measurements show that varying temperature dominates the global deformation and internal force changes of the supertall buildings [1-3] and long-span bridges [4-6]. Also, the temperature change potentially results in local effects such as cracking of concrete [7, 8] and interface debonding between different materials [9, 10]. In the past half century, extensive studies were devoted to the temperature related topics, which in general fall into three categories: temperature distribution [11-14], dynamic property variation [15-18], and structural responses [19-22].

According to Eurocode 1991-1-5 [23], the temperature action on a structural element can be decomposed into four constituent components: (1) uniform temperature change, (2) linearly varying temperature difference along the height, (3) linearly varying temperature difference along the width, and (4) non-linear temperature difference component. Component 1 leads to an axial deformation; components 2 and 3 induce bending curvature, but in most cases the latter is negligible compared with the former; and component 4 corresponds to self-equilibrated stress on the cross section, which does not cause global responses of the structure. The uniform temperature effect is straightforward for beams, namely, the axial thermal expansion or contraction at beam ends $\delta L_{\text{org}} = L_{\text{org}} \alpha \cdot \delta T$, where L_{org} , α , and T respectively represent the original free length, linear expansion coefficient, and temperature of the beam, and $\delta(\cdot)$ denotes the quantity change [24]. This study focuses on component 2 of simply supported and continuous beams.

Although the differential temperature induced deflection has been discussed on various beams, e.g., the scaled bridge model in Ref. [25] and several short-span bridges in Ref. [22], the previous literatures are mainly case studies, and thus generalized conclusions are not available. For example, the variation in the beam deflection with the span number is still unclear.

This study is intended to develop ~~an~~ analytical solutions to the beam deflection induced by the temperature difference across the depth with the aims: (1) to gain insights into the thermal deformation of continuous beams with any number of spans; (2) to provide a simple and precise formula to calculate the differential temperature induced beam deflection.

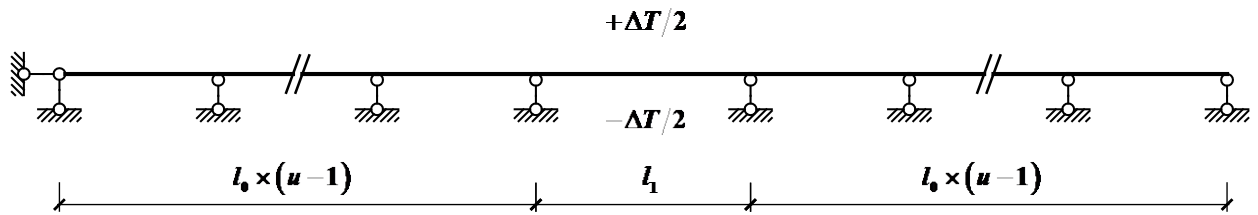
The next section presents the detailed steps of the formula development in terms of the odd- and even-numbered-span beams. Section 3 characterizes the deflection shape of beams subjected to vertical temperature difference and discusses the variation in thermal response with the structural geometry through parametric analysis. The findings of the study are summarized in the final section.

2 Formula Derivation

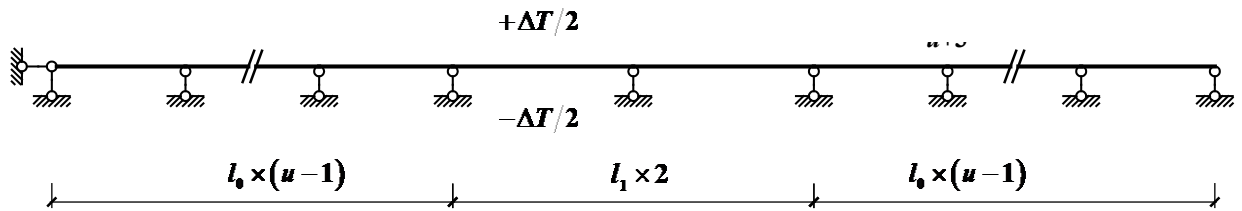
All derivations in this study are based on the classical Bernoulli–Euler beam theory. Consider a prismatic n -span beam subjected to a differential temperature change ΔT between the top and bottom surfaces, as shown in Figure 1. A positive ΔT means the top surface is warmer than the bottom. By introducing a positive integer $u = \lceil n/2 \rceil$, where $\lceil n/2 \rceil$ means the smallest integer that is not less than $n/2$, the odd- and even-numbered n can be expressed as $n = 2u - 1$ and $n = 2u$, respectively. An n -span beam has $n+1$ joints, each corresponding to a support of the beam. When the beam consists of an odd number of spans (Figure 1(a)), namely, $n = 2u - 1$, the u^{th} span is designated as the main span with a length of l_1 , while the remaining spans are identical side spans with a length of l_0 . When the beam has an even number of spans (Figure 1(b)), namely, $n = 2u$, both the u^{th} and $(u+1)^{\text{th}}$ spans are main spans, while the other spans have identical length of l_0 .

The beam has a constant cross section with the depth h and moment of inertia I , and is made up of the same material with elastic modulus E and linear expansion coefficient α . The relative flexural stiffnesses of the main and side spans are denoted as $i_1 = EI/l_1$ and $i_0 = EI/l_0$, respectively. The side-to-main span ratio is defined as $\xi = l_0/l_1$. We then have $i_1 = i_0\xi$.

The mid-span deflection of the k^{th} span beam, denoted by D_k , can be solved separately according to whether the span number n is odd or even.



(a) Span number is odd and $n = 2u - 1$



(b) Span number is even and $n = 2u$

Figure 1 Analytical model of an n -span beam

2.1 Odd-numbered n

As shown in Figure 1(a), the joints on the beam are sequentially numbered as $1, 2, \dots, 2u$ from left to right. The rotation at joint k ($1 \leq k \leq 2u$) is denoted as z_k , which is positive for a clockwise rotation. z_k can be solved by substituting the slope-deflection equations [26] into the moment equilibrium equations at each joint.

At joint 1, the moment equilibrium leads to:

$$4i_0 \cdot z_1 + 2i_0 \cdot z_2 + M_T = 0 \quad (1)$$

where M_T is the fixed-end moment caused by the temperature difference ΔT in a single span beam, and M_T is positive if it makes the bottom of the beam stretched. According to Appendix A, M_T is:

$$M_T = \frac{\alpha \cdot \Delta T}{h} EI \quad (2)$$

At joint $k = 2, 3, \dots, u-1$:

$$2i_0 \cdot z_{k-1} + 8i_0 \cdot z_k + 2i_0 \cdot z_{k+1} = 0 \quad (3)$$

At joint u :

$$2i_0 \cdot z_{u-1} + (4i_0 + 4i_1) \cdot z_u + 2i_1 \cdot z_{u+1} = 0 \quad (4)$$

Due to symmetry of both the structural configuration and temperature action, the beam deforms in a symmetric pattern, which leads to $z_k = -z_{2u+1-k}$ ($k = 1, 2, \dots, u$). Therefore, $z_{u+1} = -z_u$ and Eq. (4) becomes:

$$2i_0 \cdot z_{u-1} + (4i_0 + 2i_1) \cdot z_u = 0 \quad (5)$$

The rotation at joints $k = u+2, u+3, \dots, 2u$ can then be obtained from those at joints $k = u-1, u-2, \dots, 1$, respectively. The number of independent unknowns as well as simultaneous equations is u .

To solve for z_k ($k = 1, 2, \dots, u$), we introduce a sequence a_k with the recurrent form:

$$a_k = \frac{1}{4 - a_{k-1}} \quad (6)$$

and $a_0 = 2 - \xi$. Then Eq. (5) can be rewritten as:

$$z_u = -\frac{2i_0}{4i_0 + 2i_1} z_{u-1} = -\frac{1}{2 + \xi} z_{u-1} = -a_1 \cdot z_{u-1} \quad (7)$$

By substituting $z_u = -a_1 \cdot z_{u-1}$ into Eq. (3) with k being $u-1, u-2, \dots, 2$ in

sequence, we have the following recurrent formula:

$$z_k = -\frac{2i_0}{8i_0 - 2i_0 \cdot a_{u-k}} z_{k-1} = -\frac{1}{4 - a_{u-k}} z_{k-1} = -a_{u-k+1} \cdot z_{k-1} \quad (8)$$

According to Appendix B, the general expression of a_k ($k = 1, 2, \dots, u-1$) can be solved as:

$$a_k = \frac{\lambda_1 \varphi_1^{k-1} + \varphi_2^{k-1}}{\lambda_1 \varphi_1^k + \varphi_2^k} \quad (9)$$

where the constants $\lambda_1 = (\sqrt{3} + \xi)/(\sqrt{3} - \xi)$, $\varphi_1 = 2 + \sqrt{3}$, and $\varphi_2 = 2 - \sqrt{3}$.

By substituting $z_2 = -a_{u-1} \cdot z_1$ into Eq. (1), z_1 can be solved as:

$$z_1 = -\frac{\alpha l_0 \cdot \Delta T}{2\sqrt{3} \cdot h} \cdot \frac{\lambda_1 \varphi_1^{u-1} + \varphi_2^{u-1}}{\lambda_1 \varphi_1^{u-1} - \varphi_2^{u-1}} \quad (10)$$

Applying the recurrence relation in Eq. (8) yields

$$z_k = (-1)^k \frac{\alpha l_0 \cdot \Delta T}{2\sqrt{3} \cdot h} \cdot \frac{\lambda_1 \varphi_1^{u-k} + \varphi_2^{u-k}}{\lambda_1 \varphi_1^{u-1} - \varphi_2^{u-1}} \quad (11)$$

The above equation applies to $k = 1, 2, \dots, u$.

According to the slope-deflection equations [26], the end moments of each span beam can be expressed analytically. There is no concentrated moment acting at the joints, so the left end moment of the k^{th} ($k = 2, 3, \dots, u$) span beam is equal to the right end moment of the $(k-1)^{\text{th}}$ span beam. Therefore, we just present the joint moment, which is assumed to be positive if it stretches the beam bottom side. The moment at joint k ($k = 1, 2, \dots, u-1$) is

$$M_k = 4i_0 \cdot z_k + 2i_0 \cdot z_{k+1} + M_T = \left[1 + (-1)^k \cdot \frac{\lambda_1 \varphi_1^{u-k} - \varphi_2^{u-k}}{\lambda_1 \varphi_1^{u-1} - \varphi_2^{u-1}} \right] \cdot \frac{\alpha EI \cdot \Delta T}{h} \quad (12)$$

The moment at joint u is

$$M_u = 4i_1 \cdot z_u - 2i_1 \cdot z_u + M_T = \left[1 + (-1)^u \frac{\xi}{\sqrt{3}} \cdot \frac{\lambda_1 + 1}{\lambda_1 \varphi_1^{u-1} - \varphi_2^{u-1}} \right] \cdot \frac{\alpha EI \cdot \Delta T}{h} \quad (13)$$

Eq. (13) is the same as Eq. (12) when $k = u$. Therefore, Eq. (12) is the unified formula to calculate the joint moment for $k = 1, 2, \dots, u$. With the symmetric condition, we have $M_{2u+1-k} = M_k$ ($k = 1, 2, \dots, u$).

The downward displacement of the beam is defined to be positive. The mid-span deflection of the k^{th} ($k = 1, 2, \dots, u-1$) span beam can be calculated by the method of virtual work combined with the graphical ‘‘Product Integrals’’ method [26]:

$$\begin{aligned}
D_k &= \frac{1}{EI} \cdot \frac{l_0}{4} \cdot \frac{l_0}{2} \cdot \frac{M_k + M_{k+1}}{2} - \frac{\alpha \cdot \Delta T}{h} \frac{l_0}{2} \cdot \frac{l_0}{4} \\
&= (-1)^k \frac{\alpha l_0^2 \cdot \Delta T}{16h} \cdot \frac{(\lambda_1 \varphi_1^{u-k-1} + \varphi_2^{u-k})(1 + \sqrt{3})}{\lambda_1 \varphi_1^{u-1} - \varphi_2^{u-1}}
\end{aligned} \tag{14}$$

For the u^{th} span beam, the mid-span deflection is

$$\begin{aligned}
D_u &= \frac{1}{EI} \cdot \frac{l_1}{4} \cdot \frac{l_1}{2} \cdot \frac{M_u + M_u}{2} - \frac{\alpha \cdot \Delta T}{h} \frac{l_1}{2} \cdot \frac{l_1}{4} \\
&= (-1)^u \frac{\alpha l_0^2 \cdot \Delta T}{8\sqrt{3} \cdot \xi \cdot h} \cdot \frac{\lambda_1 + 1}{\lambda_1 \varphi_1^{u-1} - \varphi_2^{u-1}}
\end{aligned} \tag{15}$$

The symmetric condition gives the result of the $(2u-k)^{\text{th}}$ span beam as $D_{2u-k} = D_k$ ($k = 1, 2, \dots, u-1$).

Furthermore, when the main and side spans have identical span length, i.e., $\xi = 1$ and $\lambda_1 = (\sqrt{3} + 1)/(\sqrt{3} - 1) = \varphi_1$, Eqs. (14) and (15) can be unified into one formula ($k = 1, 2, \dots, u$):

$$D_k = (-1)^k \frac{\alpha l_0^2 \cdot \Delta T}{16h} \cdot \frac{(\varphi_1^{u-k} + \varphi_2^{u-k})(1 + \sqrt{3})}{\varphi_1^u - \varphi_2^{u-1}} \tag{16}$$

The formulas to calculate the joint rotation z_k (Eq. (11)), joint moment M_k (Eq. (12)), and mid-span deflection D_k (Eqs. (14)–(16)) are valid for any positive integer u . For a simply supported beam, i.e., $n = 1$ and $u = 1$, these equations generate correct results with $\xi = 1$.

2.2 Even-numbered n

For a beam with an even number of spans, as shown in Figure 1(b), the foregoing procedure in Section 2.1 can also be conducted with slight modification. The moment equilibrium equations at joint 1 and joint k ($k = 2, 3, \dots, u-1$) are identical to Eqs. (1) and (3), respectively. Due to symmetry, we have $z_k = -z_{2u+2-k}$ ($k = 1, 2, \dots, u$) and $z_{u+1} = 0$. The equilibrium equation at joint u thus becomes

$$2i_0 \cdot z_{u-1} + (4i_0 + 4i_1) \cdot z_u = 0 \tag{17}$$

The number of independent unknowns as well as simultaneous equations is also u .

Similar to the case of odd-numbered n , the relation between z_k and z_{k-1} can also be expressed by $z_k = -a_{u-k+1} \cdot z_{k-1}$ ($k = 2, 3, \dots, u$), where the sequence a_k satisfies the condition of Eq. (6) but with $a_0 = 2 - 2\xi$. From Appendix B, we have the general expression of a_k ($k = 1, 2, \dots, u-1$):

$$a_k = \frac{\lambda_2 \varphi_1^{k-1} + \varphi_2^{k-1}}{\lambda_2 \varphi_1^k + \varphi_2^k} \tag{18}$$

where the constant $\lambda_2 = (\sqrt{3} + 2\xi) / (\sqrt{3} - 2\xi)$.

Replacing λ_1 with λ_2 in Eq. (11), we obtain the joint rotation for the even-numbered n case:

$$z_k = (-1)^k \frac{\alpha l_0 \cdot \Delta T}{2\sqrt{3} \cdot h} \cdot \frac{\lambda_2 \varphi_1^{u-k} + \varphi_2^{u-k}}{\lambda_2 \varphi_1^{u-1} - \varphi_2^{u-1}} \quad (19)$$

where $k = 1, 2, \dots, u$.

According to the slope-deflection equations, the joint moment at joint k ($k = 1, 2, \dots, u$) is

$$M_k = 4i_0 \cdot z_k + 2i_0 \cdot z_{k+1} + M_T = \left[1 + (-1)^k \cdot \frac{\lambda_2 \varphi_1^{u-k} - \varphi_2^{u-k}}{\lambda_2 \varphi_1^{u-1} - \varphi_2^{u-1}} \right] \cdot \frac{\alpha EI \cdot \Delta T}{h} \quad (20)$$

and at joint $u+1$:

$$M_{u+1} = -2i_1 \cdot z_u - 4i_1 \cdot z_{u+1} + M_T = \left[1 + (-1)^{u+1} \frac{\xi}{\sqrt{3}} \cdot \frac{\lambda_2 + 1}{\lambda_2 \cdot \varphi_1^{u-1} - \varphi_2^{u-1}} \right] \cdot \frac{\alpha EI \cdot \Delta T}{h} \quad (21)$$

Due to symmetry, we have $M_{2u+2-k} = M_k$ ($k = 1, 2, \dots, u$).

The mid-span deflection of the k^{th} ($k = 1, 2, \dots, u-1$) span beam is similarly calculated as:

$$\begin{aligned} D_k &= \frac{1}{EI} \cdot \frac{l_0}{4} \cdot \frac{l_0}{2} \cdot \frac{M_k + M_{k+1}}{2} - \frac{\alpha \cdot \Delta T}{h} \cdot \frac{l_0}{2} \cdot \frac{l_0}{4} \\ &= (-1)^k \frac{\alpha l_0^2 \cdot \Delta T}{16h} \cdot \frac{(\lambda_2 \varphi_1^{u-k-1} + \varphi_2^{u-k})(1 + \sqrt{3})}{\lambda_2 \varphi_1^{u-1} - \varphi_2^{u-1}} \end{aligned} \quad (22)$$

and for the u^{th} span beam:

$$\begin{aligned} D_u &= \frac{1}{EI} \cdot \frac{l_1}{4} \cdot \frac{l_1}{2} \cdot \frac{M_u + M_{u+1}}{2} - \frac{\alpha \cdot \Delta T}{h} \cdot \frac{l_1}{2} \cdot \frac{l_1}{4} \\ &= (-1)^u \frac{\alpha l_0^2 \cdot \Delta T}{16\sqrt{3} \cdot \xi \cdot h} \cdot \frac{\lambda_2 + 1}{\lambda_2 \varphi_1^{u-1} - \varphi_2^{u-1}} \end{aligned} \quad (23)$$

The symmetric condition leads to $D_{2u+1-k} = D_k$ ($k = 1, 2, \dots, u$).

Furthermore, when the main and side spans are equal in length, i.e., $\xi = 1$ and $\lambda_2 = (\sqrt{3} + 2) / (\sqrt{3} - 2) = -\varphi_1^2$, the joint moment at joint k has a unified formula for $k = 1, 2, \dots, u+1$:

$$M_k = \left[1 + (-1)^k \cdot \frac{\varphi_1^{u-k+1} + \varphi_2^{u-k+1}}{\varphi_1^u + \varphi_2^u} \right] \cdot \frac{\alpha EI \cdot \Delta T}{h} \quad (24)$$

So does the mid-span deflection of the k^{th} span beam for $k = 1, 2, \dots, u$:

$$D_k = (-1)^k \frac{\alpha l_0^2 \cdot \Delta T}{16h} \cdot \frac{(\varphi_1^{u-k} - \varphi_2^{u-k+1})(1 + \sqrt{3})}{\varphi_1^u + \varphi_2^u} \quad (25)$$

Also, Eq. (19) applies to $k = u+1$ as it produces $z_{k+1} = 0$ at $\xi = 1$.

For a two-span continuous beam, i.e., $n = 2$ and $u = 1$, the above formulas for calculating the

joint rotation, joint moment, and mid-span deflection are still valid with $\xi = 1$.

3 Parametric analysis and discussions

This section discusses the physical meanings of the derived [formulasequations](#) in Section 2 through parametric analysis. As the beam deforms symmetrically, we focus on the left half structure only.

3.1 Contributing factors

Since the beams consisting of an odd or even number of spans correspond to different formulas, the parity of the span number n matters. Besides, the beam deformation and moment are also closely related to the material properties, structural geometry, and temperature difference.

From Eqs. (11), (12), (14), (15), and (19)–(23), the joint rotation z_k , joint moment M_k , and mid-span deflection D_k are directly proportional to the linear expansion coefficient α and temperature difference ΔT , but inversely proportional to the beam depth h . The temperature dependent rotation z_k and deflection D_k are independent of the flexural stiffness EI , and in proportion to l_0 and l_0^2 , respectively.

The joint moment M_k has no relation with the absolute value of the span length, but depends on the span length ratio ξ implicitly, which is incorporated in the parameters λ_1 and λ_2 . Meanwhile, M_k is directly proportional to EI , which implies that the strain ε of the beam is independent of EI as a result of $\varepsilon \propto M_k / (EI)$.

These temperature difference induced responses of the beam (the joint rotation, moment, strain, and deflection) differ from the external force induced responses. In general, the force induced global deformation or local strain in a beam is inversely proportional to the flexural stiffness, while the internal moment not. Therefore, the temperature difference action has different characteristics from the force action.

Additionally, z_k , M_k , and D_k also vary with the ordinal number k , cardinal number u , and span ratio ξ . For brevity, the dependency of D_k on k , u , and ξ is investigated in Sections 3.3 to 3.5.

3.2 Deflection shape

The deflection direction of the k^{th} span beam depends on the sign of D_k . Assuming a positive

temperature difference ($\Delta T > 0$), the sign of D_k is only determined by the leading term $(-1)^k$ or $(-1)^u$ in Eqs. (14), (15), (22), and (23). To prove this statement, we can define a quadratic function $f_1(x)$ as

$$f_1(x) = (x+1)(x \cdot \varphi_1^{u-1} - \varphi_2^{u-1}) \quad (26)$$

where $u \geq 1$. The roots of $f_1(x) = 0$ are $x_1 = -1$ and $x_2 = \varphi_2^{2(u-1)}$ (as $\varphi_1 = \varphi_2^{-1}$). As $\varphi_2 = 2 - \sqrt{3} \approx 0.268 < 1$, we have $0 < x_2 \leq 1$. As $\varphi_1 = 2 + \sqrt{3} > 0$, the graph of $f_1(x)$ is a parabola opening upward. Therefore, $f_1(x) > 0$ outside the region $x \in [-1, 1]$.

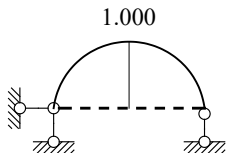
On the other hand, recalling $\lambda_1 = (\sqrt{3} + \xi)/(\sqrt{3} - \xi)$ and $\lambda_2 = (\sqrt{3} + 2\xi)/(\sqrt{3} - 2\xi)$, we have $|\lambda_1| > 1$ and $|\lambda_2| > 1$ with $\xi > 0$. As a result, $f_1(\lambda_1) > 0$ and $f_1(\lambda_2) > 0$, which imply that the fractions $(\lambda_1 + 1)/(\lambda_1 \cdot \varphi_1^{u-1} - \varphi_2^{u-1})$ and $(\lambda_2 + 1)/(\lambda_2 \cdot \varphi_1^{u-1} - \varphi_2^{u-1})$ in Eqs. (15) and (23) are positive, and the sign of D_k is solely dependent on $(-1)^u$.

Likewise, we introduce the following quadratic function $f_2(x)$:

$$f_2(x) = (x \cdot \varphi_1^{u-k-1} + \varphi_2^{u-k})(x \cdot \varphi_1^{u-1} - \varphi_2^{u-1}) \quad (27)$$

The roots of $f_2(x)$ are $x_1 = -\varphi_2^{2(u-k)-1}$ and $x_2 = \varphi_2^{2(u-1)}$. As $u \geq 1$ and $0 < \varphi_2 < 1$, we have $-1 < -\varphi_2 \leq x_1 < 0 < x_2 \leq 1$ for $k = 1, 2, \dots, u-1$, and $f_2(x)$ corresponds to a similar parabola as that of $f_1(x)$. When $|x| > 1$, $f_2(x) > 0$, so $f_2(\lambda_1) > 0$ and $f_2(\lambda_2) > 0$. Consequently, the fractions $(\lambda_1 \cdot \varphi_1^{u-k-1} + \varphi_2^{u-k})/(\lambda_1 \cdot \varphi_1^{u-1} - \varphi_2^{u-1})$ and $(\lambda_2 \cdot \varphi_1^{u-k-1} + \varphi_2^{u-k})/(\lambda_2 \cdot \varphi_1^{u-1} - \varphi_2^{u-1})$ in Eqs. (14) and (22) are always larger than zero, and the sign of D_k is determined by $(-1)^k$.

It can be seen from the above discussion that the positive temperature difference ΔT always induces an upward deflection in the outermost span beam ($k = 1$ and n), while the deflection shape of the middlemost span beam ($k = u$) depends on whether u is an odd or even number. From the 1st to u^{th} spans, the beams deflect upward and downward alternately, and the deflection shape of the $(u+1)^{\text{th}}$ to n^{th} span beams can be determined by symmetry condition with respect to the vertical centre line of the entire beam. Therefore, for a beam with an odd number of spans, i.e., $n = 2u - 1$, the deflection of each span is always opposite to the adjacent spans, whereas for a beam with $n = 2u$, the u^{th} and $(u+1)^{\text{th}}$ span beams deflect in identical direction but the remaining spans keep the span-by-span alternation pattern on deflection shape (Figure 2).



(a) $n = 1, u = 1$

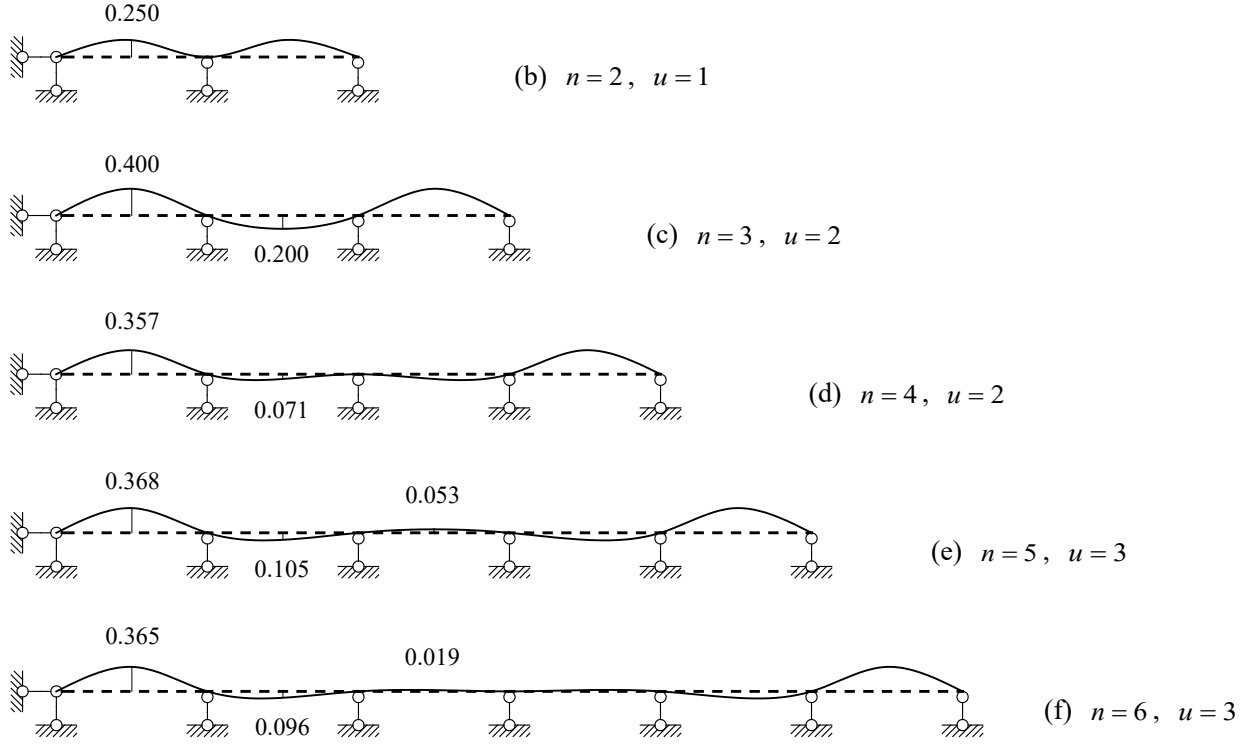


Figure 2 Thermal deflection of continuous beams with 1–6 spans ($\Delta T > 0$; $\xi = 1$; Not to scale)

3.3 Deflection magnitude of each span

To facilitate the discussion, we consider in Sections 3.3 and 3.4 that all the spans are of equal length by setting $\xi = 1$, while the influence of side-to-main span ratio ξ is investigated in Section 3.5.

When the beam consists of an odd number of spans with $\xi = 1$, the mid-span deflection of the k^{th} ($k = 1, 2, \dots, u$) span beam can be calculated by Eq. (16). Given a certain u , the deflection D_k is proportional to the item $\varphi_1^{u-k} + \varphi_2^{u-k}$. As $\varphi_2 = 1/\varphi_1$, we introduce two functions $f_3(x) = x + 1/x$ and $f_4(x) = \varphi_1^{u-x}$ to define a composite function, which produces $f_3(f_4(k)) = \varphi_1^{u-k} + \varphi_2^{u-k}$. For $k = 1, 2, \dots, u$, $f_4(k)$ decreases with increasing k and $f_4(k) \geq 1$. Meanwhile, the derivative of $f_3(x)$ is $f_3'(x) = 1 - 1/x^2$, which is positive for $x \geq 1$. Consequently, $f_3(x)$ is a monotonically increasing function in the region. As a result, the composite function $f_3(f_4(k))$ decreases as k increases, which means the outermost span ($k = 1$) and the middlemost span ($k = u$) respectively have the largest and smallest magnitudes of the mid-span deflection.

When the beam contains an even number of spans of equal length, the mid-span deflection D_k is proportional to the item $\varphi_1^{u-k} - \varphi_2^{u-k+1}$, as shown in Eq. (25). In this regard, a new function

$f_5(x) = x - \varphi_2/x$ is introduced and composed with $f_4(x) = \varphi_1^{u-x}$, and then we have $f_5(f_4(k)) = \varphi_1^{u-k} - \varphi_2^{u-k+1}$. As aforementioned, for $k=1, 2, \dots, u$, $f_4(k)$ is a monotonically decreasing function and $f_4(k) \geq 1$, whereas the derivative of $f_5(x)$ is $f_5'(x) = 1 + \varphi_2/x^2 > 0$. Therefore, the composite function $f_5(f_4(k))$ decreases with the increase of k , indicating that the outermost span beam experiences the largest thermal deflection at mid-span and the middlemost span has the least. This finding is consistent with that for the beams with odd-numbered spans.

The rotational restraints on the beam end significantly affect the beam deflection. The outermost joint receives the least rotational restraints, and thus the outermost span has the largest deflection.

3.4 Influence of number of spans on deflection magnitude

This section examines the deflection of the 1st and u^{th} span beams in terms of u . The discussion still focuses on beams with equal spans.

When the span number n is odd, substituting $k=1$ into Eq. (16) gives the largest deflection of all spans:

$$D_1^{\text{odd}} = -\frac{\alpha l_0^2 \cdot \Delta T}{16h} \cdot \frac{(\varphi_1^{u-1} + \varphi_2^{u-1})(1 + \sqrt{3})}{\varphi_1^u - \varphi_2^{u-1}} = \frac{(\sqrt{3}-1)}{2} \cdot \left(1 + \frac{\varphi_1+1}{\varphi_1^{2u-1}-1}\right) D_0 \quad (28)$$

where $D_0 = -\alpha l_0^2 \cdot \Delta T / (8h)$ represents the mid-span deflection of a simply supported beam with the span l_0 , depth h , linear expansion coefficient α , and temperature difference ΔT . From Eq. (28), the magnitude of D_1^{odd} , i.e., $|D_1^{\text{odd}}|$, becomes smaller with the increase of u . This is attributed to the rotational restraint on the right end of the 1st span beam due to the additional spans.

When n is even, the largest deflection can be found by substituting $k=1$ into Eq. (25):

$$D_1^{\text{even}} = -\frac{\alpha l_0^2 \cdot \Delta T}{16h} \cdot \frac{(\varphi_1^{u-1} - \varphi_2^u)(1 + \sqrt{3})}{\varphi_1^u + \varphi_2^u} = \frac{(\sqrt{3}-1)}{2} \cdot \left(1 - \frac{\varphi_1+1}{\varphi_1^{2u}+1}\right) D_0 \quad (29)$$

In contrary to the case of odd-numbered n , $|D_1^{\text{even}}|$ becomes larger as u increases. This is because the deflection of the beam is symmetric about the middlemost support $u+1$. Therefore, the support is equivalent to a fixed support without any rotation. With the increase of u , the outermost span is far away from the fixed support and is less restrained against rotation from the latter. The span thus deflects more.

As u approaches infinity, D_1^{odd} and D_1^{even} converge, though in opposite directions, to the same value:

$$D_1^{\text{lim}} = \frac{(\sqrt{3}-1)}{2} D_0 \quad (30)$$

Therefore, D_0 and $D_1^{\text{lim}} \approx 0.366D_0$ are respectively the upper and lower limits of the 1st span deflection of odd-numbered-span beams; while D_1^{lim} and $D_0/4$ are the corresponding limits of even-numbered-span beams. The conclusions are illustrated in Figure 2. An interesting observation is that both D_1^{odd} and D_1^{even} are a rational number multiple of D_0 (see Appendix C), whereas their limit D_1^{lim} is an irrational number times D_0 .

Similarly, the deflection of the middlemost span can be obtained by substituting $k = u$ into Eqs. (16) and (25), which represents the smallest mid-span deflection of all spans:

$$D_u^{\text{odd}} = (-1)^u \frac{\alpha l_0^2 \cdot \Delta T}{8h} \cdot \frac{(1+\sqrt{3})}{\varphi_1^u - \varphi_2^{u-1}} = (-1)^{u-1} \frac{(1+\sqrt{3})}{\varphi_1^u - \varphi_2^{u-1}} \cdot D_0 \quad (31)$$

$$D_u^{\text{even}} = (-1)^u \frac{\alpha l_0^2 \cdot \Delta T}{8h} \cdot \frac{1}{\varphi_1^u + \varphi_2^u} = (-1)^{u-1} \frac{1}{\varphi_1^u + \varphi_2^u} \cdot D_0 \quad (32)$$

It can be observed that both $|D_u^{\text{odd}}|$ and $|D_u^{\text{even}}|$ decrease monotonically with the increase of u , and they approach to zero as u goes infinity. Therefore, the limit of the u^{th} span beam deflection at mid-span is zero. This indicates that as $u \rightarrow +\infty$, the middlemost span is actually equivalent to a fixed-end beam that has no thermal deflection under the vertical temperature difference (see Figure A1(a) in Appendix A).

In fact, the convergence of D_1 and D_u to their limits is fairly quick. The deflection ratio of the outermost span beam, denoted as D_1/D_0 , can be obtained from Eqs. (28) and (29). It is a function of the span number n , as shown in Figure 3. When $n \geq 5$ or $u \geq 3$, the oscillation in D_1/D_0 is almost invisible, thereby demonstrating a quick convergence.

For the middlemost span, the absolute value of the deflection ratio $|D_u/D_0|$ can be derived from Eqs. (31) and (32). Figure 3 shows that $|D_u/D_0|$ converges to zero quickly in a monotonically decreasing manner as n increases.

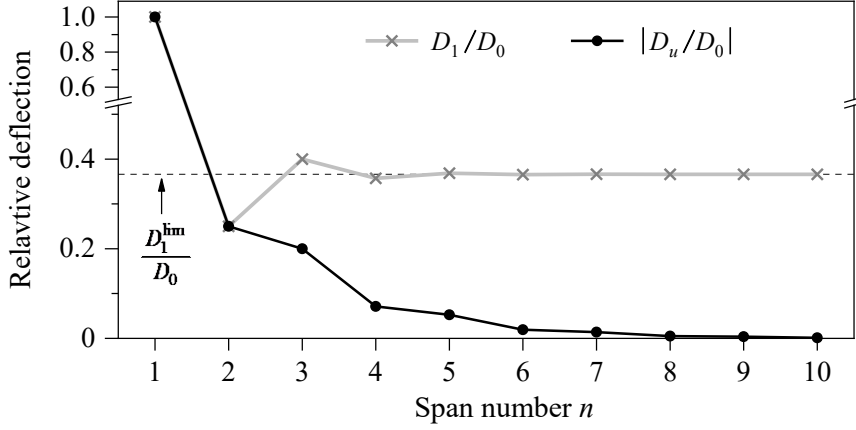


Figure 3 Variation in relative deflection of the 1st and u^{th} spans with span number n

3.5 Influence of ξ on deflection magnitude

Due to the quick convergence of the thermal deflection with the increasing span number, we consider the beams with $u = 2$, i.e., the 3-span and 4-span beams, as examples to investigate the influence of the side-to-main span ratio ξ on the deflection magnitude. In this regard, $k = 1$ corresponds to the side span, while $k = 2$ represents the main span.

By substituting $k = 1$, $u = 2$, and $\lambda_1 = (\sqrt{3} + \xi)/(\sqrt{3} - \xi)$ into Eq. (14), we obtain the side-span deflection $D_1^{n=3}$ for the 3-span beam:

$$D_1^{n=3} = -\frac{\alpha l_0^2 \cdot \Delta T}{16h} \cdot \frac{(\lambda_1 + \varphi_2)(1 + \sqrt{3})}{\lambda_1 \varphi_1 - \varphi_2} = -\frac{\alpha l_0^2 \cdot \Delta T}{16h} \cdot \frac{\xi + 3}{2\xi + 3} = D_0 \cdot \frac{1}{4} \left(1 + \frac{3}{2\xi + 3} \right) \quad (33)$$

Here, we assume the side span length l_0 is a constant, while the main span length $l_1 = l_0/\xi$ varies with ξ . From Eq. (33), the magnitude of $D_1^{n=3}$ decreases with the increase of ξ with the following limits:

$$\lim_{\xi \rightarrow 0^+} D_1^{n=3} = \frac{D_0}{2} \quad (34)$$

$$\lim_{\xi \rightarrow +\infty} D_1^{n=3} = \frac{D_0}{4} \quad (35)$$

$\xi \rightarrow +\infty$ means that the main span length is negligible. In this situation, the beam deforms like a 2-span beam, and the main span can be regarded as a fixed support to restrain the end rotation of the side span beam. This is equivalent to Figure 2(b).

For the main span deflection, substituting $k = 2$, $u = 2$, and $\lambda_1 = (\sqrt{3} + \xi)/(\sqrt{3} - \xi)$ into Eq. (15) yields:

$$D_2^{n=3} = \frac{\alpha l_0^2 \cdot \Delta T}{8\sqrt{3} \cdot \xi \cdot h} \cdot \frac{\lambda_1 + 1}{\lambda_1 \varphi_1 - \varphi_2} = \frac{\alpha l_1^2 \cdot \Delta T}{8h} \cdot \frac{\xi^2}{(2\xi + 3)\xi} = -D_{0(l_1)} \cdot \frac{1}{2} \left(1 - \frac{3}{2\xi + 3} \right) \quad (36)$$

where $D_{0(l_1)} = -\alpha l_1^2 \cdot \Delta T / (8h)$ represents the mid-span deflection of a simply supported beam of span l_1 . Here, the main span length l_1 is assumed to be a constant, and the side span length $l_0 = \xi \cdot l_1$ varies with ξ . From Eq. (36), $D_2^{n=3}$ increases with the increase of ξ , and approaches to zero and $-D_{0(l_1)}/2$ respectively as $\xi \rightarrow 0^+$ and $\xi \rightarrow +\infty$.

Based on Eqs. (33) and (36), the deflection ratio of the side to main spans is found to depend on the side-to-main span ratio ξ only, i.e.:

$$\frac{D_1^{n=3}}{D_2^{n=3}} = -\frac{(\xi + 3) \cdot \xi}{2} \quad (37)$$

As ξ is always greater than 0, the magnitude of the deflection ratio $|D_1^{n=3}/D_2^{n=3}|$ exhibits quadratic growth with ξ .

For the 4-span beam, the relation between $D_1^{n=4}$ or $D_2^{n=4}$ and ξ have the same expressions as Eqs. (33)(33) and (36)(36) except replacing ξ by 2ξ .

$$D_1^{n=4} = -\frac{\alpha l_0^2 \cdot \Delta T}{16h} \cdot \frac{(\lambda_2 + \varphi_2)(1 + \sqrt{3})}{\lambda_2 \varphi_1 - \varphi_2} = D_0 \cdot \frac{1}{4} \left(1 + \frac{3}{4\xi + 3} \right) \quad (38)$$

$$D_2^{n=4} = \frac{\alpha l_0^2 \cdot \Delta T}{16\sqrt{3} \cdot \xi \cdot h} \cdot \frac{\lambda_2 + 1}{\lambda_2 \varphi_1 - \varphi_2} = -D_{0(l_1)} \cdot \frac{1}{2} \left(1 - \frac{3}{4\xi + 3} \right) \quad (39)$$

Therefore, $D_1^{n=4}$ and $D_2^{n=4}$ ~~possessexhibit~~ similar characteristics as their counterparts for 3-span beams with the variation in ξ . The corresponding side-to-main-span deflection ratio can be calculated by $D_1^{n=4}/D_2^{n=4} = -(2\xi + 3) \cdot \xi$. As ξ increases, the magnitude of $D_1^{n=4}/D_2^{n=4}$ increases approximately four times as fast as $|D_1^{n=3}/D_2^{n=3}|$ does.

3.6 Comparisoneed with beam deflection limits

This section compares the thermal deflection of beams with the design limits to discuss the relative influence of temperature effects. According to Section 3.4, the maximum possible thermal deflection in equal-span beams is $D_0 = -\alpha l_0^2 \cdot \Delta T / (8h)$, which corresponds to a simply supported beam. D_0 can be rewritten as a dimensionless parameter as:

$$\frac{D_0}{l_0} = -\frac{1}{8} \alpha \cdot \Delta T \cdot \frac{l_0}{h} \quad (40)$$

where D_0/l_0 is the deflection-to-span ratio and l_0/h is the span-to-depth ratio. A typical value of l_0/h in bridges is around 20 [27]. With $l_0/h = 20$, Eq. (40)(39) leads to $D_0/l_0 = 2.5\alpha \cdot \Delta T$. As the thermal expansion coefficient α is in the order of $10^{-5} \text{ }^\circ\text{C}^{-1}$ and the temperature difference ΔT for bridges is generally about $10 \text{ }^\circ\text{C}$, the temperature difference-induced deflection of beams is in the order 10^{-4} of the span length.

The bridge serviceability usually defines a maximum acceptable deflection-to-span ratio of about 10^{-3} [27], which is much larger than the thermal effects. However, if such a maximum deflection is assumed to result from progressive accumulation of deterioration in bridges during a long operational period, e.g., over 10 years, then the annual change rate of the deflection would be comparable with the temperature-induced one [22]. In this respect, the thermal deflection must be taken into consideration in order to track the long-term evolution of bridge deflection.

Additionally, the maximum allowable deflection during the serviceability limit state of beams is determined for extremely overloaded cases, rather than the actual operation. Therefore, the live load effects during normal operational conditions and the temperature effects can be comparable. In this situation, the temperature effect must be considered to quantify the live load effects correctly.

4 Conclusions

This paper derives explicit solutions to the temperature difference induced deflection of a prismatic beam with any number of spans. Based on the parametric analysis, the following conclusions can be drawn.

(1) ~~The thermal deformation, including the deflection, rotation, and strain, is independent of the absolute value of the beam flexural stiffness; however, the temperature related moment is directly proportional to EI . All the concerned thermal responses are directly proportional to $\alpha \cdot \Delta T/h$. The temperature and force induced responses have different dependency on structural properties. The parity of the span number n has significant influence on the thermal behaviour of beam structures. The thermal responses of the odd- and even-numbered-span beams in this study are respectively dependent on the dimensionless parameters $\lambda_1 = (\sqrt{3} + \xi)/(\sqrt{3} - \xi)$ and $\lambda_2 = (\sqrt{3} + 2\xi)/(\sqrt{3} - 2\xi)$.~~

(2) For a prismatic beam with n spans, the thermal deflection is symmetric about the centreline of the entire structure. For the 1st to u^{th} spans, each span beam bends oppositely to its adjacent spans, and the 1st span always moves upward under the positive temperature difference. The deflection shape of the $(u+1)^{\text{th}}$ to n^{th} spans can be determined by symmetry condition.

(3) For an equal-span beam, the outermost (1^{st} or n^{th}) span has the largest thermal deflection of all spans. For odd-numbered-span beams, the mid-span deflection D_1 of the outermost span decreases from D_0 to $D_0 \cdot (\sqrt{3} - 1)/2$ as u increases from 1 to $+\infty$; whereas for even-numbered-span beams, D_1 increases from $D_0/4$ to $D_0 \cdot (\sqrt{3} - 1)/2$ with the increasing u .

(4) For an n -span beam of equal spans, the middlemost span has the smallest deflection of all spans ($n \geq 3$), and its deflection at mid-span converges quickly to zero as n increases.

The analytical formulas proposed in this study are of both theoretical and practical values. They provide not only deep insights into the fundamental relation between thermal deflection and structural properties, but also a convenient way to calculate the thermal deformation of beams. The influence of shear deformations in the Timoshenko beams deserves a further study.

Acknowledgments

This research was supported by the Hong Kong Polytechnic University (Project No. ZE1F), the Hong Kong Scholars Program (Grant No. XJ2018062), and the Interdisciplinary Research Project for Young Teachers of USTB (Fundamental Research Funds for the Central Universities) (Grant No. FRF-IDRY-19-030).

Declaration of Competing Interest

The authors declare that they have no known competing financial interests or personal relationships that could have appeared to influence the work reported in this paper.

Authorship Contributions

Yi ZHOU: Conceptualization, Methodology, Formal analysis, Investigation, Writing - original draft.

Yong XIA: Validation, Investigation, Writing - review & editing. **Yozo FUJINO:** Supervision.

Appendix A

This part derives the fixed-end moments of a beam subjected to the temperature difference ΔT across the depth, as shown in Figure A1(a). The beam has a constant cross section along the length with the span, depth, moment of inertia, elastic modulus, and linear expansion coefficient being L , h , I , E , and α , respectively.

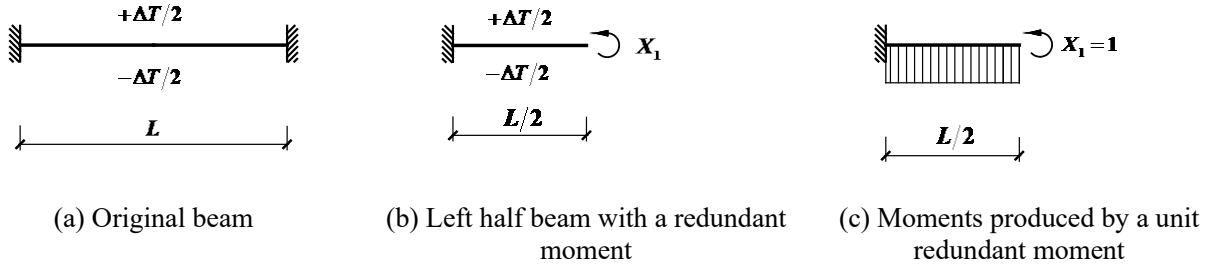


Figure A1 Analytical model of a fixed-end beam subjected to temperature difference ΔT

Taking advantage of symmetry, the left half of the original beam is considered, which is a cantilever beam of length $L/2$. With the axial deformation neglected, the mid-span moment denoted as X_1 is the only redundant for the cantilever beam in Figure A1(b). Here, the moment stretching the beam bottom is assumed to be positive. Under the action of the temperature difference ΔT and the redundant moment X_1 , the slope of the cantilever beam at the free end is zero.

By the flexibility method (also known as the force method), the compatibility equation of the cantilever beam is written as

$$\delta_{11}X_1 + \Delta_{1P} = 0 \quad (\text{A1})$$

where the flexibility coefficient δ_{11} can be evaluated using the virtual work method by applying a unit virtual moment $X_1 = 1$, as shown in Figure A1(c):

$$\delta_{11} = \frac{1}{EI} \cdot 1 \cdot \frac{L}{2} \cdot 1 = \frac{L}{2EI} \quad (\text{A2})$$

and Δ_{1P} is the free-end slope produced by the temperature difference ΔT :

$$\Delta_{1P} = \frac{\alpha \cdot \Delta T}{h} \left(-\frac{L}{2} \cdot 1 \right) = -\frac{\alpha L \cdot \Delta T}{2h} \quad (\text{A3})$$

The redundant moment X_1 is solved from Eq. (A1) as

$$X_1 = -\Delta_{1P} / \delta_{11} = \frac{\alpha \cdot \Delta T}{h} EI \quad (\text{A4})$$

X_1 is equal to the fixed-end moment of the beam in Figure A1(a), which is independent of span L .

In fact, the fixed-fixed beam in Figure A1(a) has no deformation but is subject to a constant moment X_1 along the span.

Appendix B

This part derives the general formula of a_k , which has the following recurrence relation:

$$a_k = \frac{1}{4 - a_{k-1}} \quad (\text{B1})$$

Subtracting a constant φ from both sides of Eq. (B1) yields:

$$a_k - \varphi = \frac{1}{4 - a_{k-1}} - \varphi \quad (\text{B2})$$

The right hand side of Eq. (B2) is equivalent to

$$\frac{1}{4 - a_{k-1}} - \varphi = \frac{1 - \varphi(4 - a_{k-1})}{4 - a_{k-1}} = \frac{\varphi a_{k-1} + 1 - 4\varphi}{4 - a_{k-1}} = \frac{\varphi(a_{k-1} - \varphi) + 1 - 4\varphi + \varphi^2}{4 - a_{k-1}} \quad (\text{B3})$$

Let $1 - 4\varphi + \varphi^2 = 0$, and the solutions to this quadratic equation are $\varphi_1 = 2 + \sqrt{3}$ and $\varphi_2 = 2 - \sqrt{3}$.

According to Eqs. (B2) and (B3), we obtain the following two equations:

$$a_k - \varphi_1 = \frac{\varphi_1(a_{k-1} - \varphi_1)}{4 - a_{k-1}} \quad (\text{B4})$$

$$a_k - \varphi_2 = \frac{\varphi_2(a_{k-1} - \varphi_2)}{4 - a_{k-1}} \quad (\text{B5})$$

Dividing Eq. (B4) by Eq. (B5) leads to

$$\frac{a_k - \varphi_1}{a_k - \varphi_2} = \frac{\varphi_1}{\varphi_2} \cdot \frac{a_{k-1} - \varphi_1}{a_{k-1} - \varphi_2} \quad (\text{B6})$$

Therefore, the sequence $(a_k - \varphi_1)/(a_k - \varphi_2)$ is a geometric sequence with common ratio φ_1/φ_2 . As the initial value is $(a_0 - \varphi_1)/(a_0 - \varphi_2)$, the k^{th} term of this geometric sequence is

$$\frac{a_k - \varphi_1}{a_k - \varphi_2} = \left(\frac{\varphi_1}{\varphi_2} \right)^k \cdot \frac{a_0 - \varphi_1}{a_0 - \varphi_2} \quad (\text{B7})$$

For odd-numbered-span beams, $a_0 = 2 - \xi$ and a_k can be solved from Eq. (B7) as

$$a_k = \frac{\lambda_1 \varphi_1^{k-1} + \varphi_2^{k-1}}{\lambda_1 \varphi_1^k + \varphi_2^k} \quad (\text{B8})$$

where $\lambda_1 = (\sqrt{3} + \xi)/(\sqrt{3} - \xi)$. As $a_0 = 2 - 2\xi$ for even-numbered-span beams, a_k becomes

$$a_k = \frac{\lambda_2 \varphi_1^{k-1} + \varphi_2^{k-1}}{\lambda_2 \varphi_1^k + \varphi_2^k} \quad (\text{B9})$$

where $\lambda_2 = (\sqrt{3} + 2\xi) / (\sqrt{3} - 2\xi)$.

Appendix C

This part demonstrates that Eqs. (16) and (25) produce the results in the form of $c \cdot D_0$, where c is a rational number.

Eq. (16) can be rewritten as:

$$\begin{aligned} D_k &= (-1)^k \frac{\alpha l_0^2 \cdot \Delta T}{16h} \cdot \frac{(\varphi_1^{u-k} + \varphi_2^{u-k})(1 + \sqrt{3})}{\varphi_1^u - \varphi_2^{u-1}} = (-1)^{k-1} \frac{D_0}{2} \cdot \frac{(\varphi_1^{u-k} + \varphi_2^{u-k})(1 + \sqrt{3})(1 - \varphi_2)}{(\varphi_1^u - \varphi_2^{u-1}) \cdot (1 - \varphi_2)} \\ &= (-1)^{k-1} D_0 \cdot \frac{\varphi_1^{u-k} + \varphi_2^{u-k}}{(\varphi_1^u + \varphi_2^u) - (\varphi_1^{u-1} + \varphi_2^{u-1})} \end{aligned} \quad (C1)$$

Note that $(1 + \sqrt{3})(1 - \varphi_2) = 2$ in Eq. (C1). The binomial expansion of the item $\varphi_1^u + \varphi_2^u$ gives:

$$\varphi_1^u + \varphi_2^u = (2 + \sqrt{3})^u + (2 - \sqrt{3})^u = \sum_{j=0}^u 2^{u-j} \cdot (\sqrt{3})^j + \sum_{j=0}^u 2^{u-j} \cdot (-\sqrt{3})^j \quad (C2)$$

In Eq. (C2), when j is odd, the $(\sqrt{3})^j$ and $(-\sqrt{3})^j$ related items cancel out; when j is even, both $(\sqrt{3})^j$ and $(-\sqrt{3})^j$ are integers. Consequently, $\varphi_1^u + \varphi_2^u$ produces an integer. Similarly, the items $\varphi_1^{u-k} + \varphi_2^{u-k}$ and $\varphi_1^{u-1} + \varphi_2^{u-1}$ in Eq. (C1) are also integers, which means the coefficient of D_0 is a ratio of integers, i.e., a rational number.

Likewise, Eq. (25) can be rewritten as:

$$\begin{aligned} D_k &= (-1)^k \frac{\alpha l_0^2 \cdot \Delta T}{16h} \cdot \frac{(\varphi_1^{u-k} - \varphi_2^{u-k+1})(1 + \sqrt{3})}{\varphi_1^u + \varphi_2^u} = (-1)^{k-1} \frac{D_0}{2} \cdot \frac{(\varphi_1^{u-k} - \varphi_2^{u-k+1})(\varphi_1 - 1)}{\varphi_1^u + \varphi_2^u} \\ &= (-1)^{k-1} \frac{D_0}{2} \cdot \frac{(\varphi_1^{u-k+1} + \varphi_2^{u-k+1}) - (\varphi_1^{u-k} + \varphi_2^{u-k})}{\varphi_1^u + \varphi_2^u} \end{aligned} \quad (C3)$$

Similarly, the coefficient of D_0 in Eq. (C3) is also a rational number.

References

- [1] Su JZ, Xia Y, Zhu LD, Zhu HP, Ni YQ. Typhoon- and temperature-induced quasi-static responses of a supertall structure. *ENG STRUCT.* 2017; 14391-100.
- [2] Breuer P, Chmielewski T, Górski P, Konopka E, Tarczyński L. The Stuttgart TV Tower — displacement of the top caused by the effects of sun and wind. *ENG STRUCT.* 2008; 302771-81.
- [3] Su JZ, Xia Y, Weng S. Review on field monitoring of high-rise structures. *STRUCT CONTROL HLTH MONIT.* 2020; e2629.

- [4] Zhou Y, Sun L. A comprehensive study of the thermal response of a long-span cable-stayed bridge: From monitoring phenomena to underlying mechanisms. *MECH SYST SIGNAL PR.* 2019; 124330-48.
- [5] Brownjohn JMW, Koo K, Scullion A, List D. Operational deformations in long-span bridges. *STRUCT INFRASTRUCTURE E.* 2015; 11556-74.
- [6] Xu YL, Chen B, Ng CL, Wong KY, Chan WY. Monitoring temperature effect on a long suspension bridge. *STRUCT CONTROL HLTH MONIT.* 2010; 17632-53.
- [7] Cooke N, Priestley MJN, Thurston SJ. Analysis and design of partially prestressed concrete bridges under thermal loading. *PCI J.* 1984; 2993-115.
- [8] Rojas E, Barr PJ, Halling MW. *Bridge Response Due to Temperature Variations.* Logan, UT 84332: Center for Advanced Infrastructure & Transportation, Rutgers University, 2014.
- [9] Liu J, Liu Y, Zhang C, Zhao Q, Lyu Y, Jiang L. Temperature action and effect of concrete-filled steel tubular bridges: A review. *Journal of Traffic and Transportation Engineering (English Edition).* 2020; 7174-91.
- [10] Gao WY, Teng JG, Dai J. Effect of temperature variation on the full-range behavior of FRP-to-concrete bonded joints. *J COMPOS CONSTR.* 2012; 16671-83.
- [11] Branco FA, Mendes PA. Thermal actions for concrete bridge design. *J STRUCT ENG.* 1993; 1192313-31.
- [12] Au F, Cheung SK, Tham LG. Design thermal loading for composite bridges in tropical region. *STEEL COMPOS STRUCT.* 2002; 441-60.
- [13] Zhou G, Yi T. Thermal load in large-scale bridges: A state-of-the-art review. *INT J DISTRIBUTED SENS N.* 2013; 217983.
- [14] Xue J, Lin J, Briseghella B, Tabatabai H, Chen B. Solar radiation parameters for assessing temperature distributions on bridge cross-sections. *APPL SCI.* 2018; 8627.
- [15] Xia Y, Chen B, Weng S, Ni Y, Xu Y. Temperature effect on vibration properties of civil structures: A literature review and case studies. *J CIVIL STRUCT HEALTH.* 2012; 229-46.
- [16] Zhou G, Yi T. A summary review of correlations between temperatures and vibration properties of long-span bridges. *MATH PROBL ENG.* 2014; 638209.
- [17] Mao JX, Wang H, Feng DM, Tao TY, Zheng WZ. Investigation of dynamic properties of long-span cable-stayed bridges based on one-year monitoring data under normal operating condition. *STRUCT CONTROL HLTH MONIT.* 2018; e2146.
- [18] Zhou Y, Sun L. Effects of environmental and operational actions on the modal frequency variations of a sea-crossing bridge: A periodicity perspective. *MECH SYST SIGNAL PR.* 2019; 131505-23.
- [19] Dilger WH, Ghali A, Chan M, Cheung MS, Maes MA. Temperature stresses in composite box girder bridges. *J STRUCT ENG.* 1983; 1091460-78.
- [20] Ni Y, Xia H, Wong K, Ko J. In-service condition assessment of bridge deck using long-term monitoring data of strain response. *J BRIDGE ENG.* 2011; 17876-85.
- [21] Moorthy S, Roeder C. Temperature-dependent bridge movements. *J STRUCT ENG.* 1992; 1181090-105.
- [22] Burdet OL. Thermal effects in the long-term monitoring of bridges. IABSE Symposium Report. Venice: International Association for Bridge and Structural Engineering, 2010. p. 62-8.
- [23] European Committee for Standardization (CEN). *Eurocode 1: Actions on Structures - Part 1-5: General Actions - Thermal Actions.* EN 1991-1-5:2003E. Brussels, Belgium. 2003.
- [24] Roeder C. Proposed design method for thermal bridge movements. *J BRIDGE ENG.* 2003; 812-9.
- [25] Kulprapha N, Warnitchai P. Structural health monitoring of continuous prestressed concrete bridges using ambient thermal responses. *ENG STRUCT.* 2012; 4020-38.
- [26] Leet KM, Uang C, Lanning JT, Gilbert AM. *Fundamentals of Structural Analysis.* 5th ed. New York, NY 10121:

McGraw-Hill Education, 2018.

[27] American Association of State Highway and Transportation Officials. AASHTO LRFD Bridge Design Specifications. 5th ed. Washington, D.C. 2001. 2010.